Visualizing Eigenstates of Nanotransistors with Arbitrary Shape

Douglas J. Mason

I. Introduction

Developing a thorough understanding of physical data from simulated systems have proven a difficult task. In the field of quantum chemistry large software packages have been devloped, for instance the highly-sophisticated Visual Molecular Dynamics (VMD) software which is freely available[William Humphrey and Schulten(1996)]. These packages are ideal for three-dimensional visualization of molecular orbitals, but have a substantial learning curve to use and are not pedagogically aimed. Regardless, the value of such visualization to understanding the results of a quantum simulation that can quickly respond to user input has been thoroughly studied and validated. The reader is encouraged to examine a summary of such findings in[Baker(1972)], [Small(1983)], [Kim K. Baldridge(1995)], [Hsin-Kai Wu(2004)].

The development of this project is highly personal, and as such does not fall easily under general categories of visualization research. Its aim is to facilitate visualizing the results of a research project ongoing at the Molecular Foundry at Lawrence Berkeley National Labs, serving to validate the algorithm underlying the project, and to allow the user to easily explore properties of finite two-dimensional systems. We call the final product the Eigenstate Explorer. As such, this paper will begin by explaining the theory underlying the data being examined. I will then describe the user-interface designed interact with the underlying data, and conclude with remarks on the algorithms used to create the visualizations apart from the algorithms used to derived the data being visualized.

II. Project Motivation and Background

Recent experiments conducted on single layers of carbon known as graphene have grown increasingly complex with regards to geometry. They have stepped outside the realm of linear, rectangular MOSFET-type devices and into fully two-dimensional geometries with multiple leads at arbitrary angles (see, for instance, [Y. Zhang and Kim(2006)], [B. Huard and Goldhaber-Gordon(2007)], [Y.-W. Tan and Kim(2007)]). Challenges to graphene fabrication give even linear devices substantial two-dimensional character, largely due to unpredictable defects in the etching process (see, for instance, the irregular geometries depicted in [B. Ozyilmax and Kim(2007)], [F. Sols and Neto(2007)]). The current gap between theory and experiment in the literature can be attributed to the lack of efficient tools to handle such arbitrary devices at the nano- and meso-scopic scales. This project aims to provide one such tool and demonstrate its use on proposed and potentially useful hexagonal junctions.

The underlying theory behind this project is described as single-electron coherent transport. The theory assumes that you have a finite system, in this case a small two-dimensional sheet of graphite known as graphene, which is connected to two or more infinite leads. The single electron enters through the input lead, scatters off the eigenvalues (or eigenstates) of the system, and emerges from the output lead. What we observe as experimentalists are the consequences of this scattering. First, we can observe the charge density of the device with a scanning tunneling microscope. This is described by the local density of states (LDOS) which describes the likelihood of the single electron existing at a point in the device when it enters the system with a particular energy. Second, we can observe the conductance across the device which is described by the electron transmission coefficient. While these theories are constructed using a single electron which interacts without ballistic scattering, the behavior of the single electron is assumed to be true of all electrons that enter the system. Thus they predict bulk properties of electricity for small devices where electron interaction is not an important factor.

The key ingredient to all calculations is the Hamiltonian which completely describes the system. We invert the Hamiltonian to obtain the Green's function matrix, whose diagonal and boundary blocks are used to calculate the LDOS and electronic transmission respectively. The algorithm employed here utilizes features of the Hamiltonian to obtain these results efficiently and automatically, and is currently being submitted for publication. For the purposes of this paper, we will withhold detailed information about the algorithm and instead provide a summary of how the observable quantities are calculated.

A. LDOS and Transmission

The LDOS and transmission matrix are derived from the Green's function matrix defined by

$$G_D(E) = ((E - i\eta) \cdot \mathbb{I}_D - H_D)^{-1}$$

Here H_D is the Hamiltonian chosen to represent the system and $E - i\eta$ is the Fermi energy subtracting a small imaginary parameter designed to avoid poles in the complex plane. The quantity $\mathbb{I}_D$ is the identity matrix with the size of H_D. In the tight-binding approximation, the diagonal entries of H_D will give the onsite energy of each atomic orbital and the off-diagonal elements will give the hopping potential between

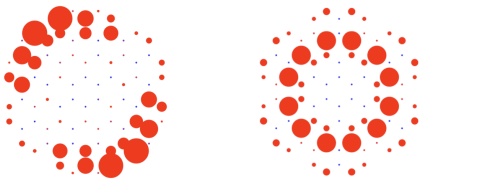

Figure 1. Eigenstates of a hexagonal graphene device

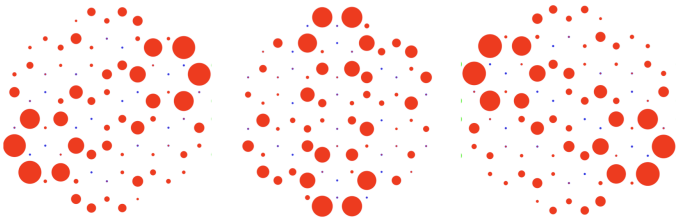

Figure 2. Different representations of an eigenstate in a hexagonal device with discrete rotational symmetry at $\theta = n\pi/3$. The above plots are given for unitary transformations at $\theta = 0, \pi/3 + \epsilon, 2\pi/3$. The system appears rotated by an angle of $\pi/3$ between each representation. While the second representation appears rotated compared to the first, since the the theta parameter is not precisely a symmetry rotation, the rotation analogy breaks down. In the continuum limit where the rotational symmetry occurs for any theta, these in-between states are always full rotations.

neighboring orbitals. Using this formalism, we can identify the density operator as

$$\hat{\rho}\left(E\right) = \frac{1}{\pi}\text{Im}\left[G_D\left(E\right)\right]$$

which has the same dimensionality as the Green's function. Similarly, we can write the local density of states as

$$LDOS(E, x) = \rho\left(E, x\right)$$

where we have dropped the hat-operational notation since now the quantity in question is a scalar. In words, if we have discretized space into a finite set of N points at positions $x(n)$ we can write the density function of an orbital at point $x(n)$ as the diagonal of the density operator at entry (n, n). Similarly, we can write the total density of states, written simply as DOS, as the spatial sum of the LDOS, or in equations

$$DOS\left(E\right) = \text{Trace}\hat{\rho}\left(E\right)$$

The transmission matrix is calculated not from entries of G along the diagonal but from the block off-diagonal elements communicating information from the input to the output boundaries, which we define as $G_{\text{In}\to\text{Out}}$. We assume that we have obtained the self-energies for all boundaries, and define gamma matrices from the self-energy of the input and output boundaries such that $\Gamma_{\text{In(Out)}} = 2\text{Im}\left[\Sigma_{\text{In(Out)}}\right]$. We apply the Lippman-Schwinger equation to compute the transmission matrix

$$\hat{T}(E) = \Gamma_{\text{In}}(E)G^{*}_{\text{In}\to\text{Out}}(E)\Gamma_{\text{Out}}(E)G_{\text{In}\to\text{Out}}(E)$$

and the transmission coefficient $T(E) = \text{Trace}\hat{T}(E)$

B. Eigenstates

The key concept to this project derives from a feature of all Hermitian matrices like the Hamiltonian to be diagonalized into eigenstates and eigenenergies using the formula

$$H = Q^T DQ$$

where the Q matrix provides the eigenstates

$$Q = [\psi_1, \psi_2, \dots]$$

and the D matrix provides the eigenenergies

$$D = \begin{bmatrix} E_1 & & & \\ & E_2 & & \\ & & \ddots & \\ & & & E_n \end{bmatrix}$$

By decomposing the Hamiltonian into its eigenstates, that is, the columns of the Q matrix, we can explore which energies the electrons are scattering off to produce the results that interest us. The above images plot the density $\rho_i\left(x\right) = \left|\psi_i(x)\right|^2$ for three eigenstates each of which is associated with an eigenenergy. These states are important to understand since they illuminate how the geometry of the device enhances or disrupts electron transmission.

C. Eigensubspaces

The key quantity to quantum scattering are not the eigenstates by are the eigenenergies. For most Hamiltonians, the two are indistinguishable, as each eigenstate ψ_i is associated with a unique eigenenergy E_i. When a system exhibits symmetry, however, there are linearly dependent vectors in the Hamiltonian which break this one-to-one relationship. In these cases, an eigenenergy can be associated with multiple eigenstates with different electron densities in the device. In the case of the two-dimensional systems explored in this study, rotational or reflection symmetry will cause eigenenergies to connect to either one or two eigenstates. In the latter case, a true visualization of the electron density requires us to consider all possible unitary transformations between the two eigenstates. Using the rotational unitary transformation, which relies on only one parameter we conveniently call θ, we write

$$\psi_\theta\left(x\right) = \psi_1 \cos\theta + \psi_2 \sin\theta$$

For this eigenenergy, all possible $\psi_\theta(x)$ where $\theta \in [0, 2\pi]$ are equally valid representations of the scattering state. For a system which has discrete rotational symmetry, the meaning of θ can be interpreted as an actual rotation of the eigenstate. However, it only takes this meaning at the rotational angle that produces the symmetry, at angles in-between the symmetry angles it is instead a mixture of the two states with no obvious analogy.

D. Partial Density of States (PDOS)

Since the basis of eigenstates is as valid as a spatial basis, we can decompose the DOS into a sum of partial densities of states (PDOS) from each eigenstate as

$$DOS\left(E\right) = \sum_{n=1}^{N} PDOS\left(E, n\right)$$

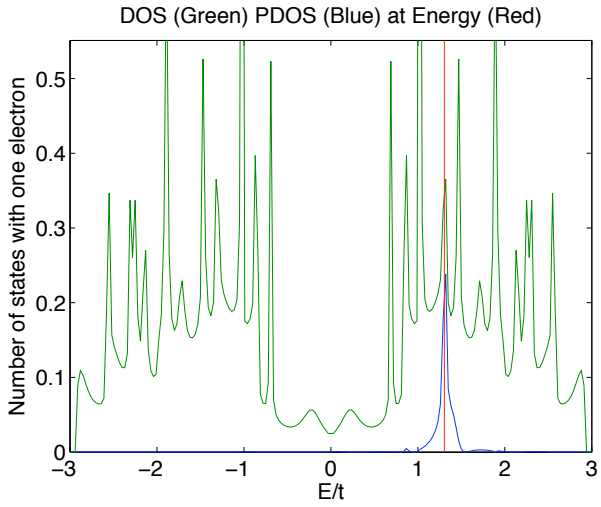

Figure 3. DOS (green), PDOS (blue), for eigenstate at eigenenergy (red). The PDOS is a function always smaller than the DOS which can take on different shapes for different eigenstates

where

$$PDOS\,(E,n) = \psi_n^* \hat{\rho}(E) \psi_n$$

and where the asterisk demarks the conjugate transpose. In theoretical chemistry, the PDOS of the highest-energy occupied molecular orbital (HOMO) and the lowest-energy unoccupied molecular orbital are crucial quantities that have acquired full subdisciplines for their study.

E. Eigenenergy Decomposition

The density operator for a device not connected to leads is described by a set of delta-functions

$$\hat{\rho}_{\text{closed}}\,(E) = \sum_{i=1}^{N} \psi_i \psi_i^* \delta\,(E - E_i)$$

and thus

$$\text{DOS}_{\text{closed}}(E) = \sum_{i=1}^{N} \delta\,(E - E_i)$$

since $|\psi_i|^2$ is normalized to one over all space. In the extreme example of a system with one degree of freedom, say a single atom with an orbital of energy E_0 we can write this as

$$\hat{\rho}_0\,(E) = \psi_0 \psi_0^* \delta(E - E_0)$$

Attaching a lead to this atom, but say putting it in an infinite line of atoms broadens the density operator as a Lorentzian defined by

$$\hat{\rho}_{0,\text{open}}(E) = \psi_0 \psi_0^* \frac{1}{2\pi} \frac{\Gamma}{\left(\frac{\Gamma}{2}\right)^2 + (E - E_0)^2}$$

where Γ is the coupling energy between the atoms in the chain. Visually, this broadens the delta function with a width Γ and which preserves the area under the curve.

Connecting leads to a device with many eigenstates, however, mixes and broadens these delta functions in unpredictable ways to produce the LDOS we observe in a nanotransistor.

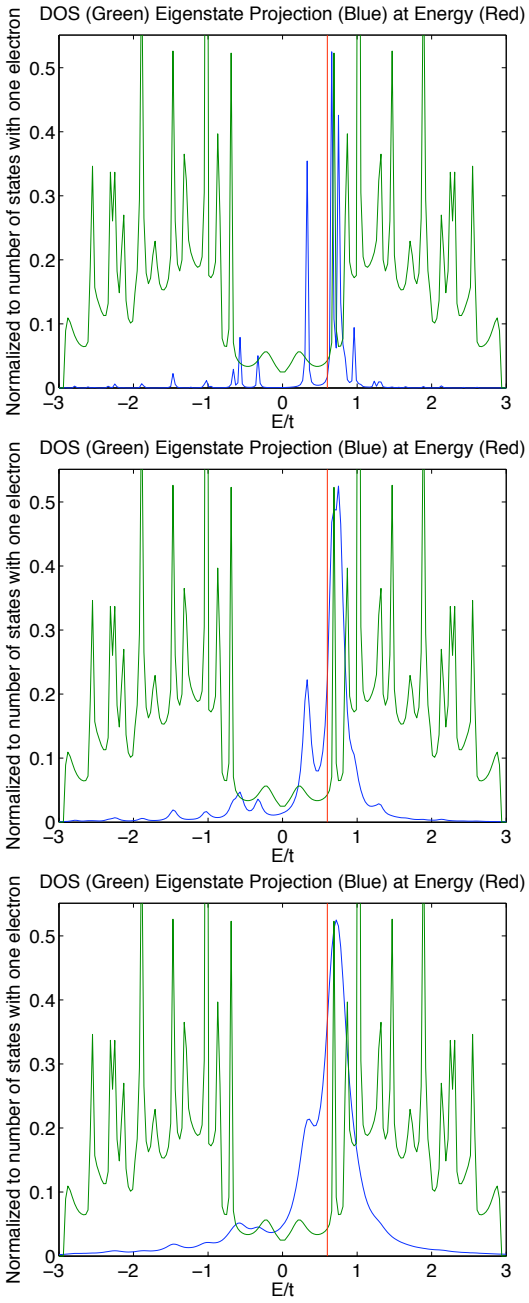

Figure 4. DOS (green), Eigenenergy cecomposition (blue), inquiry energy E_0 (red) plotted with increasing values of Γ from left-to-right demonstrating the value of adjusting this parameter for visualization aid. For small values, distinctions between the eigenvalues are clear, but it is difficult to see. For large values, the function is very easy to see, but detail is lost.

This occurs much in the same way that cutting a hole into a resonating cavity will cause energy to leak and the sound to change. This phenomenon is used to produce most wind instruments and the analogy between the nanotransistor and a flute is very instructive. In the former, we allow an electron to enter the system and we observe how it emerges, having scattered off the eigenvalues (and eigenstates) of the device. In the latter, you provide energy to the flute by blowing against the lip, this energy scatters off of resonant modes of the flute, and emerges as a sound wave through the holes of the

instrument. Just as an artisan wants to design a flute with a high-quality sound and to produce particular tones by adjusting the hole size and position, as well as the material of the flute, as physicists we want to adjust the conductance properties of the transistor by adjusting the lead width and the transistor geometry. This is why examining the eigenstates of the system and how they contribute to the "sound", that is the transmission and LDOS, is so valuable.

We can decompose the LDOS into the eigenstates of the system in a manner similar to PDOS. In the perspective of the eigenenergy decomposition, however, instead of looking at how a single eigenstate contributes to the DOS over all energies, we are interested in how all the eigenstates contribute to the LDOS at a particular energy. We write the correlation coefficient simply as

$$C_i\left(E\right) = \text{PDOS}(E, i)$$

Once we have calculated the correlation vector, we are challenged with visualizing a discrete set of quantities that correlate to a discrete set of energies with extrinsic meaning. It is desirable to plot these quantities against the DOS which is a function of energy, and it would be tempting to plot them a series of delta functions in analogy with the closed DOS. These are nearly impossible to visualize since the delta functions may overlap or approach each other at arbitrarily small distances. Incorporating information about the correlation coefficient further complicates the visualization. We instead make an analogy between the complex full system and the simple one-atom system with one eigenstate connected to the atom chain. In this case, we convolve the delta functions with a Lorentzian of arbitrary width Γ and sum the result in the equation

$$f(E, E_0) = \frac{1}{2\pi}\sum_i C_i(E_0)\frac{\Gamma}{\left(\frac{\Gamma}{2}\right)^2 + \left(E - E_i\right)^2}$$

The results are plotted in the accompanying figure.

F. Analogy between density operator $\hat{\rho}(E)$ and transmission operator $\hat{T}(E)$

The above formulations provide deep insight into the phenomena behind the density operator. There remains however a need to explore the transmission operator at the same level. Physics have developed a quantity known as the spectral operator

$$\hat{A} = G^*_{\text{In}\to\text{Out}}(E)\Gamma_{\text{Out}}(E)G_{\text{In}\to\text{Out}}(E) = \Gamma^{-1}_{\text{In}}(E)\hat{T}(E)$$

which provides information on how the scattering states of the device contribute to the measured conductance. It is dependent on the overlap between the eigenstates that the electron excites and the boundary region of the output lead. This can be easily understood since if the electron scatters off of a state that does not allow it to couple to the output lead and exit the system, then it cannot transmit across the device. We can replace all the above formulas that utilize the density operator $\hat{\rho}(E)$ with the spectral operator $\hat{A}(E)$ to obtain parallel information about

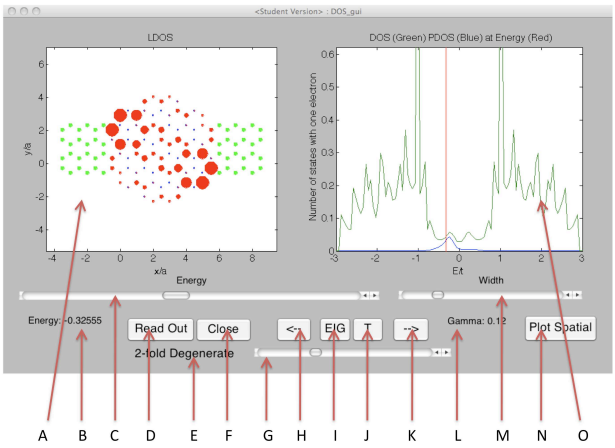

Figure 5. Graphical user-interace for the Eigenexplorer. A) Eigenstate/LDOS spatial plot. B) Energy indicator. C) Energy slider. D) Read out button. E) Degeneracy indicator. F) Close button. G) Degeneracy rotation slider. H) Move to next lowest-energy eigenstate. I) Eigenstate/LDOS toggle. J) Transmission/LDOS toggle. K) Move to next highest-energy eigenstate. L) Gamma indicator. M) Gamma slider. N) Spatial plot toggle. O) Eigenstate decomposition/Partial DOS plot.

the transmission functions. We summarize the results in the following set of equations

$$\text{PTrans}\left(E, n\right) = \psi^*_n\hat{A}(E)\psi_n$$

$$\text{LTrans}(E, x) = A(E, x)$$

$$T\left(E\right) = \Gamma_{\text{in}\to\text{out}}\sum_{n=1}^{N}\text{PTrans}\left(E, n\right)$$

$$C^T_i\left(E\right) = \text{PTrans}(E, i)$$

$$f_T(E, E_0) = \frac{1}{2\pi}\sum_i A_i(E_0)\frac{\Gamma}{\left(\frac{\Gamma}{2}\right)^2 + \left(E - E_i\right)^2}$$

III. User Interface

The user-interface is designed to provide intuitive controls of the eigenstate, LDOS, and electron transmission data. It is centered around correlating information in space as well as observables for the experimentalist. We call it the Eigenstate Explorer.

The Eigenstate Explorer's main features are two large plots, one on the left that plots the spatial information being examined, and one on the right which provides detailed information about the density of states or transmission which would be observed in an experiment. In it's default state, it plots the LDOS on the left at a random electron energy and plots the eigenstate decomposition on the right.

The interface has three toggle buttons, the Eigenstate/LDOS toggle, the DOS/T toggle, and the Spatial Plot toggle, the first two of which toggle the interface between different modes of operation. In the Eigenstate mode, the left side plots the electron density for an individual eigenstate or representation

of the eigensubspace. The eigenstate is chosen to correlate the with eigenenergy closest to the energy selected by the energy slider. If the user clicks either the left or right arrow button, the eigenstate correlating to the next lowest or highest energy is then selected. The right side plots the PDOS or the PTrans of the eigenstate, which is chosen by the DOS/T toggle. In the LDOS mode, the left side plots the LDOS or the LTrans at the energy selected by the energy slider, chosen by the DOS/T toggle. The right side then plots the eigenenergy decomposition at that energy. The Spatial Plot toggle allows the user to stop the computer from plotting the spatial information, which can significantly increase the performance of the computer. This can be useful for dragging the energy slider to see how the eigenstate decomposition changes continuously.

In the eigenstate mode, if the system has identified that the eigenvalue being examined has two degenerate eigenstates in its eigensubspace (see earlier for explanation) it updates the degeneracy indicator and activates the eigensubspace rotation slider. The user is then allowed to adjust the θ parameter between 0 and 2π as the spatial plot updates concurrently. For a degenerate eigensubspace, the definition of the PDOS and the PTrans is actually the simple sum of the PDOS and the PTrans for the two eigenstates of the subspace as already defined. Thus as the user rotates in the eigensubspace, the PDOS and PTrans do not change according to θ.

IV. Visualization Algorithms

In this section I outline the various algorithms used to create the spatial and function plots of the Eigenstate Explorer user-interface.

A. Spatial Plots

The LDOS, described earlier in the paper, provides a numerical value relating the probability of a scanning tunneling microscope observing an electron at that position in space with the energy specified. The computer calculates this sequence of numbers for each point in the discretized space, then computes the average ρ and the standard deviation σ. The LDOS is then normalized so that

$$\rho(\text{LDOS}) = n_{\text{size}}$$

where n_{size} is the average circle size for the plotter. The LDOS is plotted using red circles whose size is determined by the normalized LDOS at that point. It is necessary to normalize the LDOS at each electron energy so that they can be compared for variations in their spatial pattern. In truth, the LDOS total quantity varies with DOS, which is always plotted to the right of the LDOS. If we did not normalize, however, states with a low total DOS would be invisible to the user. By providing the DOS function (with a red vertical line to demarcate the electron energy) alongside the normalized LDOS, the program is able to inform the user of *both* the subtle changes at each energy and the overall scaling.

To avoid filling the spatial plot with an extreme value which masks the rest of the plot, all points in space with a normalized LDOS above $\rho+2\sigma$ are truncated to that quantity. Their circles are plotted purple instead of red to avoid misleading the user.

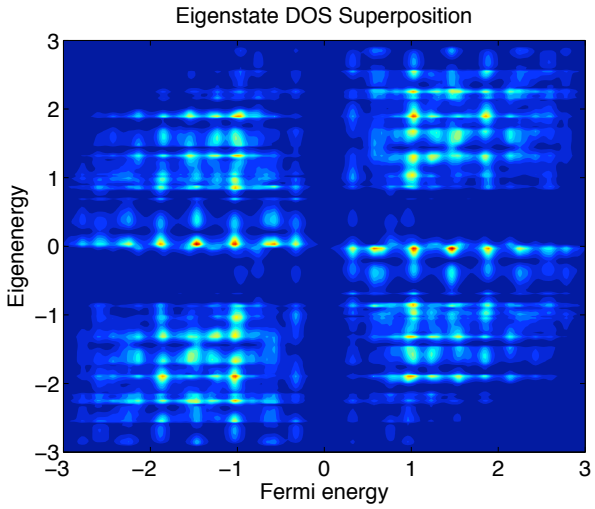

Figure 6. Two-dimensional color image of the eigenenergy decomposition function $f(E, E_0)$ where E_0 varies by the y-axis and E varies by the x-axis. Peaks along the most contributory eigenenergies are prevalent at $E = \pm 1$

When the user clicks the Eigenstate/LDOS toggle, the program enters the eigenstate mode and the spatial plot changes accordingly. In this mode, the circle sizes now reflect the quantity$\rho_i(x) = |\psi_i(x)|^2$ normalized and truncated as for the LDOS. Each eigenstate by definition is normalized, however, so there is no need to provide information about the overall scaling factor.

B. Function Plots

In both Eigenstate and DOS modes, the right hand side plots the DOS or the Trans. Since extreme values are common in these quantities as a result of Van Hove singularities, it is necessary to scale these functions so that extreme values do not overly mitigate the rest of the function. We calculate the average ρ and the standard deviation σ and set the maximum value of the y-axis to

$$y_{\max} = \min(\rho + 2\sigma, \max(\text{DOS}))$$

In the Eigenstate mode, the right-hand side plots either the PDOS or the PTrans underneath the DOS and the Trans. No scaling is added since it is scientifically meaningful to show the comparative values of the two functions. In the DOS mode, the right-hand side plots the eigenenergy decomposition of the LDOS or the LTrans along with the DOS and the Trans. In this case, the eigenenergy decomposition is scaled simply so that its largest value matches $y_{\max}$ since its overall scaling is arbitrary to begin with.

C. Two-dimensional Static Plots

Clicking the "read out" button plots the full two-dimensional information of the eigenenergy decomposition as a single color image for comparison. This can be useful for a quick summary

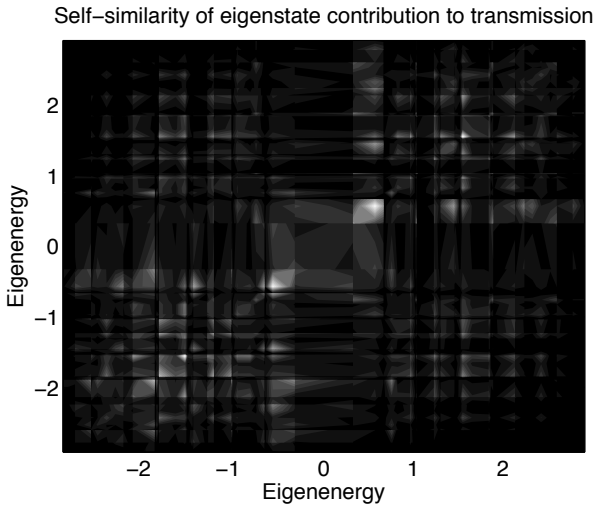

Figure 7. Two-dimensional greyscale image of the self-similarity matrix function $S_{i,j}$. Each point is plotted along the x- and y-axes by the eigenenergies of the matrix element.

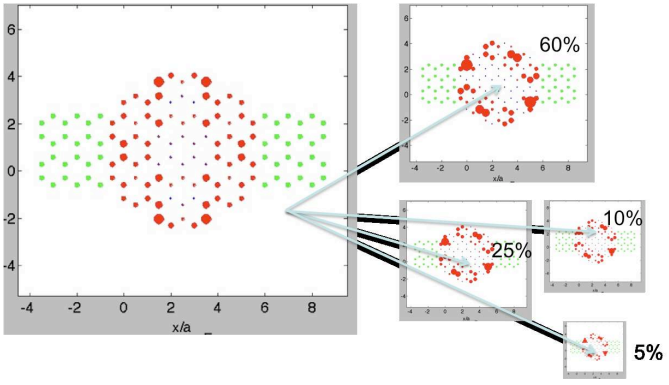

Figure 8. Proposed real-time scaling of small multiples of eigenstates to reflect relative contribution to the LDOS

of the information but poor for the detailed analysis the user-interface is designed for. The "read out" button also provides the user the transmission self-similarity matrix defined by

$$S_{i,j} = \int_{-\infty}^{\infty} C_i^T(E) \times C_j^T(E) dE$$

For each point in the above image, the eigenenergies associated with its x- and y-positions are compared for a similar transmission profile. White areas indicate eigenstates which contribute strongly and in tandem, giving an indication of underlying symmetries. In the above example, a few eigenstates at .75eV resonate strongly with a wide spectrum of other eigenenergies.

V. Conclusion and Future Work

The development of the Eigenstate Explorer has been invaluable as a learning tool for myself and as an effective research tool. It has been used to systems outside the scope of the original project, including Fabry-Perot resonators and large finite-difference matrices. It has been effective in proving the efficacy of the underlying algorithm used to efficiently calculate the LDOS and the transmission, and it is currently being used to custom-generate nanodevices with desirable transmission properties. Experimentalists at the Molecular Foundry have been recently successful in crafting large ensembles of nanodevices from graphene, and we are eager to develop a multitude of studies utilizing this tool to examine and interact with the experimental data.

There remain some future extensions of the current work. One proposal, which was actually voiced early in project development, included decomposing the LDOS into eigenstates that could be simultaneously visualized. It was suggested that the spatial scaling of the eigenstates could reflect their relative contribution to the LDOS as in the accompanying figure. The author would find such an extension visually appealing, but ultimately it was decided that such a visualization would require a large amount of work without much scientific reward.

The fate of this work is still unknown. Such visualizations in physics have never been standardized or widely published, while their value seems to be quite high. Functions such as the eigenenergy decomposition are similarly novel to the field, and finding the appropriate publication venue for it could prove difficult. However, the pedagogical value of these function is eminent. As the user scrolls through the electron energy, it is immediately obvious how localized the system is in energy, giving a strong indication of the amount of scattering throughout the system. It was a real thrill to test the Eigenstate Explorer for various extreme-example systems, and see quantum mechanical principles emerge effortlessly. Many seasoned professionals (read: Lab scientists and Berkeley physics professors) have voiced their surprise that their intuitions for these systems were surprisingly underdeveloped and have expressed an interest in their own copy of the software for personal use. We hope to publish this tool for them in the near future.

References

[B. Huard and Goldhaber-Gordon(2007)] N. Stander K. Todd B. Yang B. Huard, J. A. Sulpizio and D. Goldhaber-Gordon. Transport measurements across a tunable potential barrier in graphene. *Physical Review Letters*, 98(236803), 2007.

[B. Ozyilmax and Kim(2007)] D. Efetov B. Ozyilmax, P. Jarillo-Herrero and P. Kim. Electronic transport in locally gated graphene nanoconstrictions. *Applied Physics Letters*, 91(192107), 2007.

[Baker(1972)] Lawrence Baker, Sheldon R.; Talley. The name assigned to the document by the author. this field may also contain sub-titles, series names, and report numbers.the relationship of visualization skills to achievement in freshman chemistry. *Journal of Chemical Education*, 49(11):775–6, 1972.

[F. Sols and Neto(2007)] F. Guinea F. Sols and A. H. Castro Neto. Coulomb blockade in graphene nanoribbons. *Physical Review Letters*, 99(166803), 2007.

[Hsin-Kai Wu(2004)] Priti Shah Hsin-Kai Wu. Exploring visuospatial thinking in chemistry learning. *Science Education*, 88(3), 2004.

[Kim K. Baldridge(1995)] Jerry P. Greenberg Kim K. Baldridge. Qmview: A computational chemistry three-dimensional visualization tool at the interface between molecules and mankind. *Journal of Molecular Graphics*, 13(1):63–66, 1995.

[Small(1983)] Mary E. Small, Melinda Y.; Morton. The name assigned to the document by the author. this field may also contain sub-titles, series names, and report numbers.research in college science teaching: Spatial visualization training improves performance in organic chemistry. *Journal of College Science Teaching*, 13(1):41–3, 1983.

[William Humphrey and Schulten(1996)] Andrew Dalke William Humphrey and Klaus Schulten. Vmd: Visual molecular dynamics. *Journal of Molecular Graphics*, 14(1):33–38, 1996.

[Y.-W. Tan and Kim(2007)] K. Bolotin Y. Zhao S. Adam-E. H. Hwang S. Das Sarma H. L. Stormer Y.-W. Tan, Y. Zhang and P. Kim. Measurement of scattering rate and minimum conductivity in graphene. *Physical Review Letters*, 99(246803), 2007.

[Y. Zhang and Kim(2006)] J. P. Small M. S. Purewal Y.-W. Tan M. Fazlollahi J. D. Chudow J. A. Jaszczak H. L. Stormer Y. Zhang, Z. Jiang and P. Kim. Landau-level splitting in graphene in high magnetic fields. *Physical Review Letters*, 96(136806), 2006.